Revisiting bevacizumab + cytotoxics scheduling using mathematical modeling: proof of concept study in experimental non-small cell lung carcinoma

Diane-Charlotte Imbs, Raouf El Cheikh, Arnaud Boyer, Joseph Ciccolini, Celine Mascaux, Bruno Lacarelle, Fabrice Barlesi, Dominique Barbolosi, Sébastien Benzekry

Revisiting bevacizumab + cytotoxics scheduling using mathematical modeling: proof of concept study in experimental non-small cell lung carcinoma

Diane-Charlotte Imbs[1*] & Raouf El Cheikh[1*], Arnaud Boyer[1,3], Joseph Ciccolini[1], Céline Mascaux[1,3], Bruno Lacarelle[1], Fabrice Barlesi[1,3], Dominique Barbolosi[1] and Sébastien Benzekry[2**]

1 : *SMARTc Unit, Inserm S_911 CRO2, Aix-Marseille University, Marseille France.*

2 : *MONC Team, Inria, Bordeaux France.*

3 *: Aix Marseille University ; Assistance Publique Hôpitaux de Marseille. Multidisciplinary Oncology & Therapeutic Innovations dpt. Marseille. France.*

[*:] These two authors contributed equally

[**] correspondence to Dr Sebastien Benzekry: sebastien.benzekry@inria.fr

Abstract

Concomitant administration of bevacizumab and pemetrexed-cisplatin is a common treatment for advanced non-squamous non-small cell lung cancer (NSCLC). Vascular normalization following bevacizumab administration may transiently enhance drug delivery, suggesting improved efficacy with sequential administration. To investigate optimal scheduling, we conducted a study in NSCLC-bearing mice using. First, experiments demonstrated improved efficacy when using sequential versus concomitant scheduling of bevacizumab and chemotherapy. Using a mathematical model of tumor growth under therapy accounting for the normalization effect, we predicted an optimal delay of 2.8 days between bevacizumab and chemotherapy. This prediction was confirmed experimentally, with reduced tumor growth of 38% as compared to concomitant scheduling, and prolonged survival (70 *vs.* 74 days). Alternate sequencing of 8 days failed in achieving similar increase in efficacy, thus emphasizing the utility of modeling support to identify optimal scheduling. The model could also be a useful tool in the clinic to personally tailor regimen sequences.

Introduction

When combined to chemotherapy, anti-VEGF-A bevacizumab achieved improved overall survival (OS) and/or progression free survival (PFS) in multiple phase III trials for several types of solid tumors (1–7). In breast cancer, bevacizumab efficacy and survival benefits remain controversial, leading the US FDA to withdraw its approval in 2011 (8).

Although the main effect of bevacizumab is the disruption of the vascularization, increased efficacy with combined administration could also be achieved from transitory vascular normalization, a paradoxical effect of antiangiogenics (9–12). Indeed, preclinical and clinical studies have shown that bevacizumab induces transient changes in the vascular architecture (9,13,14). While the unaltered tumor vasculature is tortuous, chaotic and poorly functional (15), bevacizumab prunes and remodels tumor vessels to make them resemble normal tissues in terms of structure and function (10,16). It also proved to induce a more homogeneous distribution of cytotoxics in actively proliferating areas of tumor vessels (17). Therefore, determining alternate scheduling with bevacizumab could improve efficacy (9).

In line with these hypothesis, Dickson *et. al* showed that administrating topotecan after bevacizumab to neuroblastoma tumor-bearing mice resulted in reduced tumor growth as compared with concomitant administration (18). A recent study showed that bevacizumab followed 24 hours later by paclitaxel potentiated its anti-tumor activity in ovarian cancer model (17). At bedside, Avallone *et. al* showed that administrating bevacizumab 4 days prior to chemotherapy in patients with locally advanced rectal cancer led to better OS and PFS compared to concomitant administration (19). Although promising, most attempts to revisit bevacizumab scheduling have been made

on an empirical basis and a trial-and-error mode. Mathematical modeling could help assisting experimental and clinical studies to better understand the combined effects of antiangiogenics and cytotoxics on tumor growth (20). Building on the Hahnfeldt model for the effect of antiangiogenic monotherapy (21), Wilson *et. al* developed a model to quantify the dynamics of interaction between tumor growth, vasculature generation and antiangiogenic treatment. They demonstrated a possible synergistic interaction between sunitinib and irinotecan (22). Recently, Hutchinson and colleagues developed a model of vascular tumor growth and normalization from breast cancer mice treated with bevacizumab alone (23). Still in breast cancer, our team tested multiple regimens for combining bevacizumab and paclitaxel. Experimental results combined with mathematical simulations suggested that scheduling bevacizumab 2 days before paclitaxel could improve anti-tumor efficacy and reduce metastatic spreading (24).

The aim of the present modeling and experimental study was to assess predictions from a semi-mechanistic mathematical model in terms of the optimal sequence of administration for the combination of bevacizumab and pemetrexed-cisplatin in Non-Small Cell Lung Cancer (NSCLC).

Materials and Methods

Mice experiments

Cell lines

Human NSCLC cells H460 stably transfected with luciferase (H460 Luc+) were purchased from Perkin Elmer, France. This BioWare light producing cell line was derived from the H460 human adenocarcinoma by stable transfection of the North American firefly gene expressed from the SV40 promoter. Cells were cultured per manufacturer recommendation at 37°C in a humidified atmosphere with 5% CO2. H460 Luc+ cells were regularly authenticated based on viability, growth, morphology, and *in vitro* bioluminescence measuring.

For experiment-2, tumor growth monitoring was carried-out by fluorescence. Therefore, H460 Luc+ cells were transfected with tdTomato gene using pPGK-tdTomato lentiviral plasmid lentiviral plasmid as vector kindly provided by Dr Valérie Le Morvan (Institut Bergonié, Bordeaux France). Forty-eight hours after transfection, blasticidine (10 µg/mL) was added and selection was maintained for two weeks. Resulting H460 Luc+ dtTomato+ cells were regularly authenticated by microscopy based on viability, growth, morphology, and *in vitro* fluorescence monitoring.

Animal experiments

All experiments were approved by the local ethical committee of our institution and registered as # 2015110616255292 (French Ministère de l'Education Nationale, de l'Enseignement Supérieur et de la Recherche) prior to starting the experiments. Guidelines for animal welfare in experimental oncology as recommended by European regulations were followed. Pathogen-free, immunocompromised 6-week-old female

swiss nude mice (Charles River Laboratories, France) were kept in a sterile environment for 2 weeks upon reception. Mice were maintained in sterilized filter-topped cages and a sterile thermostated cabinet throughout the study. Signs of distress, decreased physical activity and any behavioral change were monitored daily. Bodyweights were monitored twice weekly as a surrogate marker for general toxicity. Water was supplemented with paracetamol (eq. 80 mg/kg/day) to prevent any disease-related pain. Animals showing signs of distress, pain, cachexia (*i.e.*, loss of 10% of body weight), and tumor mass over 2 g (*i.e.*, approximatively 2 cm^3) were euthanized.

Xenografting

H460 Luc+ (and tdTomato+ for the second experiment) cells were trypsinized, counted, centrifuged (5 minutes, 1000g) and washed twice with sterile PBS. Cells were resuspended in RPMI-1640 with 60% Matrigel (BD Sciences France) and maintained in ice-cooled conditions until engraftment. A volume of 50 µL containing 80 000 cells (experiment-1) and 120 000 cells (experiment-2) was injected ectopically in the left flank of each mouse under anesthesia. In total, 132 tumor-bearing mice were required to perform both experiments. However, overall 139 mice were initially xenografted, to ensure that eventually at least 48 (experiment-1) + 84 mice (experiment-2) presenting positive and measurable tumors could be used, considering an estimated 5% of failure rate during the grafting procedure.

Bioluminescence imaging

In experiment-1, monitoring of primary tumor growth started one week after engraftment. Acquisitions started 12 minutes after firefly D-Luciferin (Perkin Elmer, 300 mg/kg) intra-peritoneal injection to reach a plateau in bioluminescence signaling (25). Acquisition and data processing were performed using IVIS spectrum imager equipped

with the Living Image 4.2 software (Perkin Elmer). Imaging was performed twice per week. All imaging was performed in anesthetized animals (sevoflurane).

Fluorescence imaging

In experiment-2, imaging was performed twice in anesthetized animals (sevoflurane). Acquisition (excitation: 554 nm, emission: 581 nm), and data processing were performed using IVIS spectrum imager equipped with the Living Image 4.2 software.

Experiment-1: treatments

In experiment-1, 47 xenografted mice were randomized into 4 treatment arms (Figure S1-A): control (saline injection, n = 12), sequential treatment with bevacizumab administered 4 days before pemetrexed-cisplatin ("Beva then Chemo 4 days", n = 12), sequential treatment arm with bevacizumab administrated 4 days after pemetrexed-cisplatin ("Chemo then Beva 4 days", n = 11), and a concomitant treatment arm ("Beva + Chemo", n = 12). Treatment started 17 days after xenograft. Doses in each arm were $20\ mg \cdot kg^{-1}, 100\ mg \cdot kg^{-1}$ and $3\ mg \cdot kg^{-1}$ for bevacizumab, pemetrexed and cisplatin, respectively. All treatments, including saline, were administered by intra-peritoneal route for three 14-days cycle. All animals were sacrificed on day 76 post xenografts.

Experiment-2: treatments

The second experiment was performed with model-based changes both in scheduling and sample sizes. In experiment-2, 77 xenografted mice were randomized into 5 treatment arms (Figure S1-B): control (saline injection, n = 15), sequential treatment with bevacizumab administered 3 days (see next section below) before pemetrexed-cisplatin ("Beva then Chemo 3D", n = 16), sequential treatment with bevacizumab administered 8 days before pemetrexed-cisplatin ("Beva then Chemo 8 days", n = 15),

concomitant (“Beva + Chemo”, n = 15), and pemetrexed and cisplatin alone (Chemo, n = 15). The administered doses in each arm were $20\,mg \cdot kg^{-1}, 100\,mg \cdot kg^{-1}$ and $3\,mg \cdot kg^{-1}$ for bevacizumab, pemetrexed and cisplatin, respectively. All treatments were administered by intra-peritoneal route. As for experiment-1, 3 cycles (14 days cycle) were administered, starting on day 14 after xenograft. All animals were sacrificed at the end of the experiment on day 87 post xenografts.

Pharmacokinetic/Pharmacodynamic (PK/PD) modeling

Structural Model

The tumor size at time t is denoted $V(t)$. The function $C(t)$ combines plasma concentration of pemetrexed and cisplatin ($C(t) = C_{pem}(t) + C_{cis}(t)$). The function $A(t)$ represents plasma concentrations of bevacizumab. PK time course profiles for bevacizumab, cisplatin and pemetrexed were modeled each by a one-compartment model with absorption compartment and PK parameters from the literature (26–28). Figure S2-A depicts the concentration profiles for each treatment. A scheme describing the PD model is given in Figure 1. It is based on the following hypotheses:

- (H1) Without treatment the tumor size kinetics follow a gompertzian growth governed by parameters α (proliferation rate of the tumor cells) and β (rate of exponential decrease of the tumor relative growth rate) (29).
- (H2) Cytotoxics act by targeting a fraction of the tumor size (log-kill effect) (30). This effect is driven by the parameter γ.
- (H3) There is a delay between the administration time of cytotoxics and their effects on tumor. Tumor cells pass through different stages, characterized by different degree of damages, before they get eliminated (31). The transfer rate between these stages is denoted k.

- (H4) In the absence of data monitoring the state of the tumor vasculature, the antiangiogenic effect of bevacizumab is not explicitly modeled.

(H5) Beside its antiangiogenic activity, bevacizumab increases the drugs delivery by improving the vasculature quality Q (32). The dynamics of this improvement is assumed to follow the bevacizumab concentration, delayed by a time shift τ for the normalization to occur. The magnitude of the improvement is controlled by a parameter δ.The above assumptions are translated into the following system of nonlinear ordinary differential equations:

$$\begin{cases} \frac{dV}{dt} = \left(\alpha - \beta \ln\left(\frac{V}{V_c}\right)\right) V - \gamma Q C V & V(t=0) = V_0 \\ Q(t) = 1 + \delta A(t-\tau) & \\ \frac{dZ_1}{dt} = \gamma Q C V - k Z_1 & Z_1(t=0) = 0 \\ \frac{dZ_2}{dt} = k(Z_1 - Z_2) & Z_2(t=0) = 0 \\ \frac{dZ_3}{dt} = k(Z_2 - Z_3) & Z_3(t=0) = 0 \\ N = V + Z_1 + Z_2 + Z_3 & \end{cases}$$

The initial size V_0 was set to 7.04 x 10^6 photons/second considering that 80 000 cells were injected (experiment-1) and a previously established conversion ratio of $V_c = 1$ cell ≈ 88 photons/second (33).

Statistical model and parameters estimation

For description of the inter-animal variability we used the nonlinear mixed-effects statistical framework (34). It consists in assuming a distribution of the parameters within the animal population, taken here to be lognormal for each parameter. Importantly, these were the same for all treatment groups. The structural model above depends on 6 parameters $(\alpha, \beta, \gamma, \delta, \tau, k)$. After an initial sensitivity analysis showing that not all of these parameters were identifiable from our data set, we reduced this to the 4

parameters ($\alpha, \beta, \delta, \tau$). These parameters were then estimated by adapting the result of likelihood maximization performed with the Monolix software (version 2016R1, Lixoft) using visual assessment of the goodness-of-fit (visual predictive checks) and consideration of the root mean squared error. See supplementary methods for details. Values of the resulting parameters are reported in Table 1. Model simulations were performed using Matlab.

Statistical analysis

Statistical analyses were performed using R software 3.3.2 (R Core Team, 2016). Inter-group differences in tumor growth were tested by non-parametric Kruskal-Wallis tests, should the data not meet the assumptions for one-way ANOVA. Further between-groups comparisons were performed either by Dunn's multiple comparison tests when treatment groups were compared with the control group, either by Nemenyi post-hoc tests with Tukey approximation for pairwise multiple comparison between groups. Survival analysis was done using Kaplan–Meier analysis. Inter-group differences in survival were tested for significance by the log-rank tests. Owing to sample size, a p-value <0.05 was considered statistically significant.

Results

Administrating bevacizumab before pemetrexed + cisplatin improves efficacy and median of survival

Experiment-1 efficacy

Monitoring of tumor growth for experiment-1 is shown in Figure 2-A. At the end of the treatment phase (D53), mean tumor size (expressed x 10^9 in photons/second (p/s)) were 16.9 ± 3.7 (Control), 19.2 ± 3.4 ("Chemo then Beva 4 days"), 15.4 ± 2.5 ("Beva + Chemo) and 6.9 ± 2.1 ("Beva then Chemo 4 days"). A statistical difference was found between the groups ($p = 0.012$). Further Dunn's multiple comparison tests evidenced a significant difference between the sequential administration "Beva then Chemo 4 days" and control arms (59% tumor growth reduction, $p = 0.047$). Conversely, concomitant "Beva + Chemo" and reversed "Chemo then Beva 4 days" groups had modest effects on tumor growth inhibition (9% tumor reduction $(p = 0.98)$ and 13% higher tumor size $(p = 1)$ as compared with control group respectively).The sequential administration "Beva then Chemo 4 days" also confirmed its superiority in efficacy when compared with other treatment groups (55% tumor reduction, almost reaching significance compared to "Beva + Chemo" $(p = 0.071)$ and 64% tumor reduction compared to "Chemo then Beva 4 days" $(p = 0.0073)$). All mice in the control group had to be sacrificed at D53.

At study conclusion (D67, *i.e.* 18 days after all treatments stopped), mean tumor growth (expressed x 10^9 in p/s) were 19.4 ± 3.7 ("Chemo then Beva 4 days"), 15.7 ± 2.7 ("Beva + Chemo") and 10.0 ± 2.0 ("Beva then Chemo 4 days"). The sequential administration

"Beva then Chemo 4 days" arm had the lowest mean tumor size compared with other remaining groups (36% lower than concomitant "Beva + Chemo" arm and 49% lower than reversed "Chemo then Beva 4 days" arm), although no statistical significance was reached ($p = 0.42$ and 0.13, respectively).

Experiment-1 survival

Survival curves for experiment-1 are displayed in Figure 2-B. The median survival times were 39 days (Control), 49 days ("Chemo then Beva 4 days"), 55 days ("Beva + Chemo"), and 67 days ("Beva then Chemo 4 days"). A Log-rank test showed a significant difference between all groups $(p < 0.0001)$. Further Log-rank tests showed that each treatment group was significantly different than the control arm $(p < 0.001)$. Moreover, the sequential administration "Beva then Chemo 4 days" arm had greater survival median and was significantly different than concomitant "Beva + Chemo" $(p = 0.0485)$ and reversed "Chemo then Beva 4 days" arms $(p = 0.0496)$. Conversely, no significant difference was observed between "Beva + Chemo" and "Chemo then Beva 4 days" arms $(p = 0.631)$.

Mathematical modeling predicts an optimal time delay of 3 days between the administration of bevacizumab and pemetrexed + cisplatin

The selected model is a modified version of the Gompertz model with a delay in the treatment effects (31) and inclusion of a dynamic variable Q accounting for the vasculature quality and thus, the normalization effect. See materials and methods for a detailed description of the model equation, data fit and parameters' estimation method. Population analysis yielded the median parameter and inter-animal variability

estimates reported in Table 1 with good relative standard errors. Goodness of fit was assessed by visual predictive check plots with acceptable 95% prediction confidence intervals (Figures 3A-D), which demonstrated a good agreement between the model simulations and the experimental data (see residual analysis in Figure S7). Individual simulations also demonstrated the ability of our model to reproduce individual tumor growth dynamics for each mouse (Figure S8).

Optimal delay between bevacizumab and pemetrexed + cisplatin

The model with parameters calibrated on the experiment-1 data allowed us to perform simulations varying the time lag between the administrations of bevacizumab and the pemetrexed-cisplatin doublet. The criterion for quantification of efficacy was the area under the tumor growth curve. Delays ranging from 1 to 10 days were tested. Simulation results showed that a 2.8 days delay between bevacizumab and chemotherapy achieved greater reduction in tumor sizes, with a difference of 76.8% in tumor size as compared with concomitant scheduling (Figure 4-A, -B, -C). Of note, this value is different from the delay that was used in experiment-1 (4 days). Our quantification of the normalization dynamics also predicted that a delay of 8 days would perform substantially worse, with a difference of only 54.3% as compared with concomitant administration (Figure 4-C). Quantification of the inter-animal variability of the model parameters using our population approach allowed to simulate the resulting inter-animal variability of the optimal inter-drugs administration gap. The optimal gap ranged from 0 to 10 days with median 2.8 days and standard deviation 1.84 days (Figure 4-D).

Validation of the optimal delay predicted by the model

To test the predictions from the mathematical model, we designed a new experiment that implemented the above-mentioned schedules (3 and 8 days lag for sequential administrations of “Beva then Chemo”).

Experiment-2 efficacy

Tumor growth for experiment-2 is shown in Figure 5-A. At the end of the treatment phase (D54), mean tumor size (expressed in p/s) were 12567 ± 2461 (Control), 8692 ± 543 (“Beva then Chemo 8 days”), 8446 ± 1253 (Chemo), 7486 ± 1106 (“Beva + Chemo”) and 4626 ± 868 (“Beva then Chemo 3 days”). A statistically significant difference between all arms was obtained $(p = 0.0016)$. Further Dunn’s multiple comparison tests confirmed the superiority of the sequential administration “Beva then Chemo 3 days”, and showed a statistically significant difference in efficacy between the “Beva then Chemo 3 days” arm and the control arm (63% of tumor growth reduction, $p = 0.002$). Other treatment sequences led to more modest effects on tumor growth as compared with control arm. Furthermore, mean tumor size for the sequential administration “Beva then Chemo 3 days” arm was markedly lower and almost reached significant difference compared to all other treatment arms (*i.e.*, 38% compared with concomitant “Beva + Chemo” $(p = 0.072)$, 47% tumor growth reduction as compared with “Beva then Chemo 8 days” $(p < 0.001)$, and 45% compared with Chemo group $(p = 0.016)$).

At the end of the experiment (D67, *i.e.* 9 days after all treatment stopped), a statistically significant difference was found between the 4 remaining arms $(p = 0.015)$. Further Dunn’s multiple comparison tests showed that “Beva then Chemo 8 days” was significantly different than the optimized “Beva then Chemo 3 days” group (48% tumor

growth reduction, $p = 0.007$). However, no more statistically significant difference was evidenced between the other treatment arms.

Experiment-2 survival

The median survival times were 48 days (Control), 54 days (Chemo), 67 days ("Beva then Chemo 8 days"), 70 days ("Beva + Chemo") and 74 days ("Beva then Chemo 3 days"), as presented in Figure 5-B. A log-rank test showed a statistically significant difference between each treatment arm and the Control arm ($p < 0.0001$). Consistently with our mathematical model predictions, further log-rank tests showed a statistically significant difference between "Beva then Chemo 3 days" and "Beva then Chemo 8 days" arms ($p = 0.0056$). Conversely, the difference did not reach statistical significance between sequential "Beva then Chemo 3 days" and concomitant "Beva + Chemo" arms ($p = 0.32$).

Discussion

Bevacizumab induces a transient phase of vascular normalization. If correctly identified, this could increase drug delivery and improve treatment outcome. In this study, we proposed an integrative strategy that combined experiments on NSCLC tumor bearing mice and mathematical modeling to explore and validate improved scheduling of the sequential administration of bevacizumab with cytotoxics. In our first experiment, our data confirmed the benefits, in terms of survival and efficacy, of administrating bevacizumab before cytotoxics. To analyze these data, we developed a semi-mechanistic mathematical model with a critical component quantifying the dynamics of vascular normalization. Model parameters were estimated using a nonlinear mixed effects approach and simulations predicted that administrating bevacizumab 3 days before cytotoxics would yield better efficacy. Subsequent experiments confirmed the superiority of this optimized sequence compared to other sequential and concomitant administrations. This proves that beyond a simple shift to sequential administration to achieve better efficacy, the precise timing of the administration of each drug does matter and that mathematical modeling may help to identify optimized alternate scheduling that would require too much resources to be explored empirically.

Human NSCLC H460 cells are a canonical model when performing experimental therapeutics studies in lung cancer – altogether, more than 1700 papers have been published, both in vitro and in vivo, using this very model. In this respect, we have chosen the H460 model as a paradigm for mimicking NSCLC tumors – hundreds of papers have tested a variety of drugs, alone or in combination, in nude mice bearing H460 xenografts as we did in this work – ranging from cytotoxics, targeted therapies,

biologics, nanodrugs, radiotherapy, or anti-angiogenics like bevacizumab (for bevacizumab, over the last 5 years see (35–37)).

Compared to our previous study (24), the mathematical model presented here was simplified to focus on a minimal number of equations and parameters. We abandoned a more mechanistic description of the vasculature quality in terms of stable and unstable vessels to the benefit of a more phenomenological but more parsimonious and robust model that implements normalization in terms of a simple delay from the bevacizumab concentration.

Mean tumor growth curves obtained in experiment-1 highlight the high inter-animal variability observed within each treatment group (Figure 2-A). This variability can partially explain the high residual variability ($\sigma = 0.951$). Moreover, comparing standard errors of tumor growth data between experiment-1 and -2 emphasizes the higher variability of bioluminescence measurements compared with fluorescence imaging. A likely explanation for this discrepancy is the inter-animal variability of pharmacokinetics of luciferine used as a tracer for bioluminescence (38).

In experiment-2, although differences in survival between the « Beva + Chemo » and « Beva then Chemo 3 days » groups did not reach statistical significance, median survival was still larger in the latter than in the former (74 days versus 70 days). Moreover, final tumor size was 38% smaller in the « Beva then Chemo 3 days » as compared to the « Beva + Chemo » group. The p-value of a Kruskal-Wallis test for this difference was not below the arbitrarily level of 0.05, but was close to it ($p = 0.072$), thus still supporting superiority of the « Beva then Chemo 3 days » group. We hypothesize that this lack of statistical significance in our results is due to a limited power of the study, itself linked to the restricted number of animals per group for ethical constraints.

Several studies have already explored alternate sequences for administrating antiangiogenics with other drugs, with sometimes contradictory results. Rocchetti *et al.* found that giving bevacizumab after targeted therapy in tumor-bearing mice yielded better efficacy (39). Recently, Hutchinson et al. (23) inferred – using a mathematical model and experimental data from breast cancer models – a vessel normalization window beginning 15 days after the start of antiangiogenics, thus suggesting that administrating cytotoxics 2 weeks after bevacizumab could improve efficacy, a much larger optimal delay as compared with other studies (22,24). In addition, such lag-time could hardly meet the requirements of clinical testing, because bevacizumab is usually administered on a Q2W or a Q3W basis at bedside. The optimal lag we identified in our study is in line with other experimental studies that explored the normalization window after bevacizumab or other anti-angiogenics administration, since most of these reported an optimal delay ranging between 2 and 5 days (32,40,41). In patients, Avallone and colleagues showed that administrating bevacizumab 4 days prior to chemotherapy yielded better efficacy compared to concomitant administration (19).

Intriguingly, two clinical studies in NSCLC and metastatic colorectal cancer showed reduced tumor drug delivery of cytotoxic agents when administered 1 and 4 days after bevacizumab (42), which contrasts with our preclinical findings and direct clinical observation of vessel normalization after bevacizumab administration by means of interstitial fluid pressure measurements and functional computed tomography (43). More precisely, a study conducted on n = 10 NSCLC patients treated with a single dose of 15 mg/kg of bevacizumab followed by ^{11}C labeled-docetaxel found a decreased tumor uptake of the chemotherapy after 4 days (44). These findings were obtained on a small group, with a different bevacizumab dose, no repeated cycle and a different chemotherapeutic drug than here, which altogether might explain the

discrepancy. Interestingly, in (44) a wide inter-patient variability was observed in the reduction of perfusion and uptake of docetaxel. To this regard, our mathematical model could be of help by characterizing and quantifying the tumor response in a patient-specific fashion and integrate relevant biomarkers of vessel normalization into a predictive numerical tool for an individually optimized scheduling.

Together, these findings highlight the importance of drug scheduling and advocate further studies to optimize scheduling of anti-angiogenic drugs. In this respect, our approach in conducting experimental studies assisted by semi-mechanistic mathematical modeling proved to be efficient and both time- and cost-effective. Our proof-of-concept study suggests that simplified modeling could help to address the issue of finding the optimal dosing and scheduling of anticancer treatments to improve efficacy.

In addition, our model could be used in a biomarker-based strategy for improving anti-angiogenic therapy. As observed in Figure 4-D, even in a homogenous controlled animal population, variability in the optimal gap was observed for the parameters' distribution. Although no predictive biomarker has been yet clearly validated with anti-angiogenics (45), our model parameters – possibly included in a broader modeling of metastatic disease (46) – could be quantitatively linked to imaging data and/or predictive circulating biomarkers with bevacizumab acting as covariates (47,48). Consequently, this would provide personalized simulations of response to treatment allowing to individually adapt the dose and timing in order to maximize the efficacy and reduce the toxicity.

STUDY HIGHLIGHTS

o What is the current knowledge on the topic?

Bevacizumab is usually administrated concomitantly with cytotoxics. Several studies showed that administrating bevacizumab before cytotoxics yields better efficacy by improving drug uptake. This is supported by a transient phase of vascular normalization induced by antiangiogenics administration. However, determining this best sequence is challenging and could be patient-dependent.

o What question did this study address?

What is the optimal schedule for the administration of bevacizumab and pemetrexed-cisplatin doublet in NSCLC?

o What this study adds to our knowledge?

This study shows, using experimental settings and mathematical modeling, that administrating bevacizumab 3 days before cytotoxics yields better efficacy and overall survival compared to concomitant, cytotoxics-before-bevacizumab and cytotoxics-alone treatments. It also provides a validated model that could be used to individualize combination regimen in the clinic.

o How might this change drug discovery, development, and/or therapeutics?

This proof-of-concept study demonstrates that simplified modeling could help to address the issue of finding and personalizing optimal sequences when combining anticancer treatments to improve clinical outcome.

AUTHOR CONTRIBUTIONS

S. B., A. B., J. C. R.EC. and DC. I. wrote the article.; D.B, F.B, S.B, A.B, J.C., R.EC., DC. I., B.L. and C.M. designed the research; A.B. and J.C. performed the research; D.B, S.B, A.B, J.C., R.EC., and DC.I. analyzed the data.

CONFLICTS OF INTEREST

D.B., F.B., S.B., A.B., R.EC., DC. I., C.M. and B.L declared no conflicts of interest

J.C. received fees for participating to Boards from Roche Laboratory.

ACKNOWLEDGMENTS

We thank Dr Valerie Le Morvan and Pr Jacques Robert from the Institut Bergonié, France, for their kind assistance. This study was supported by grants from Canceropole PACA, Roche Laboratory (BevaLung Project) and AM*IDEX (Mars Project, AMU). DC.I. and R.EC. post-doc positions were funded by the AM*IDEX (Mars Project, AMU) grant.

References

1. Hurwitz H, Fehrenbacher L, Novotny W, Cartwright T, Hainsworth J, Heim W, et al. Bevacizumab plus Irinotecan, Fluorouracil, and Leucovorin for Metastatic Colorectal Cancer. N Engl J Med. 2004 Jun 3;350(23):2335–42.

2. Sandler A, Gray R, Perry MC, Brahmer J, Schiller JH, Dowlati A, et al. Paclitaxel–Carboplatin Alone or with Bevacizumab for Non–Small-Cell Lung Cancer. N Engl J Med. 2006 Dec 14;355(24):2542–50.

3. Miller K, Wang M, Gralow J, Dickler M, Cobleigh M, Perez EA, et al. Paclitaxel plus Bevacizumab versus Paclitaxel Alone for Metastatic Breast Cancer. N Engl J Med. 2007 décembre;357(26):2666–76.

4. Tewari KS, Sill MW, Long HJI, Penson RT, Huang H, Ramondetta LM, et al. Improved Survival with Bevacizumab in Advanced Cervical Cancer. N Engl J Med. 2014 Feb 20;370(8):734–43.

5. Zalcman G, Mazieres J, Margery J, Greillier L, Audigier-Valette C, Moro-Sibilot D, et al. Bevacizumab for newly diagnosed pleural mesothelioma in the Mesothelioma Avastin Cisplatin Pemetrexed Study (MAPS): a randomised, controlled, open-label, phase 3 trial. The Lancet. 2016 Apr 2;387(10026):1405–14.

6. Fu P, He Y-S, Huang Q, Ding T, Cen Y-C, Zhao H-Y, et al. Bevacizumab treatment for newly diagnosed glioblastoma: Systematic review and meta-analysis of clinical trials. Mol Clin Oncol. 2016 May;4(5):833–8.

7. Perren TJ, Swart AM, Pfisterer J, Ledermann JA, Pujade-Lauraine E, Kristensen G, et al. A Phase 3 Trial of Bevacizumab in Ovarian Cancer. N Engl J Med. 2011 décembre;365(26):2484–96.

8. Li Q, Yan H, Zhao P, Yang Y, Cao B. Efficacy and Safety of Bevacizumab Combined with Chemotherapy for Managing Metastatic Breast Cancer: A Meta-Analysis of Randomized Controlled Trials. Sci Rep. 2015 Oct 27;5:15746.

9. Jain RK. Normalizing tumor vasculature with anti-angiogenic therapy: A new paradigm for combination therapy. Nat Med. 2001 Sep;7(9):987–9.

10. Jain RK. Normalizing Tumor Microenvironment to Treat Cancer: Bench to Bedside to Biomarkers. J Clin Oncol. 2013 Jun 10;31(17):2205–18.

11. Jain RK. Antiangiogenesis strategies revisited: from starving tumors to alleviating hypoxia. Cancer Cell. 2014 Nov 10;26(5):605–22.

12. Fuso Nerini I, Cesca M, Bizzaro F, Giavazzi R. Combination therapy in cancer: effects of angiogenesis inhibitors on drug pharmacokinetics and pharmacodynamics. Chin J Cancer. 2016;35:61.

13. Kerbel RS. Antiangiogenic Therapy: A Universal Chemosensitization Strategy for Cancer? Science. 2006 May 26;312(5777):1171–5.

14. Cesca M, Morosi L, Berndt A, Nerini IF, Frapolli R, Richter P, et al. Bevacizumab-Induced Inhibition of Angiogenesis Promotes a More Homogeneous Intratumoral Distribution of Paclitaxel, Improving the Antitumor Response. Mol Cancer Ther. 2015 Oct 22;15(1):125–35.

15. Carmeliet P, Jain RK. Angiogenesis in cancer and other diseases. Nature. 2000 Sep 14;407(6801):249–57.

16. Carmeliet P, Jain RK. Principles and mechanisms of vessel normalization for cancer and other angiogenic diseases. Nat Rev Drug Discov. 2011 Jun;10(6):417–27.

17. Cesca M, Morosi L, Berndt A, Nerini IF, Decio A, Zucchetti M, et al. Abstract 3377: Bevacizumab-improved distribution of paclitaxel in ovarian cancer xenografts potentiates antitumor efficacy. Cancer Res. 2016 Jul 15;76(14 Supplement):3377–3377.

18. Dickson PV, Hamner JB, Sims TL, Fraga CH, Ng CYC, Rajasekeran S, et al. Bevacizumab-Induced Transient Remodeling of the Vasculature in Neuroblastoma Xenografts Results in Improved Delivery and Efficacy of Systemically Administered Chemotherapy. Clin Cancer Res. 2007 Jul 1;13(13):3942–50.

19. Avallone A, Pecori B, Bianco F, Aloj L, Tatangelo F, Romano C, et al. Critical role of bevacizumab scheduling in combination with pre-surgical chemo-radiotherapy in MRI-defined high-risk locally advanced rectal cancer: results of the branch trial. Oncotarget. 2015 Jul 30;6(30):30394–407.

20. Ciccolini J, Benzekry S, Lacarelle B, Barbolosi D, Barlési F. Improving efficacy of the combination between antiangiogenic and chemotherapy: Time for mathematical modeling support. Proc Natl Acad Sci U S A. 2015 Jul 7;112(27):E3453.

21. Hahnfeldt P, Panigrahy D, Folkman J, Hlatky L. Tumor Development under Angiogenic Signaling. Cancer Res. 1999 Oct 1;59(19):4770–5.

22. Wilson S, Tod M, Ouerdani A, Emde A, Yarden Y, Adda Berkane A, et al. Modeling and predicting optimal treatment scheduling between the antiangiogenic drug sunitinib and irinotecan in preclinical settings. CPT Pharmacomet Syst Pharmacol. 2015 Dec;4(12):720–7.

23. Hutchinson L, Mueller H-J, Gaffney E, Maini P, Wagg J, Phipps A, et al. Modeling Longitudinal Preclinical Tumor Size Data to Identify Transient Dynamics in Tumor Response to Antiangiogenic Drugs. CPT Pharmacomet Syst Pharmacol. 2016 Nov 1;5(11):636–45.

24. Mollard S, Ciccolini J, Imbs D-C, Cheikh RE, Barbolosi D, Benzekry S, et al. Model driven optimization of antiangiogenics + cytotoxics combination: application to breast cancer mice treated with bevacizumab + paclitaxel doublet leads to reduced tumor growth and fewer metastasis. Oncotarget. 2017 Feb 18;8(14):23087–98.

25. Mollard S, Fanciullino R, Giacometti S, Serdjebi C, Benzekry S, Ciccolini J. In Vivo Bioluminescence Tomography for Monitoring Breast Tumor Growth and Metastatic Spreading: Comparative Study and Mathematical Modeling. Sci Rep. 2016 Nov 4;6:36173.

26. Johnsson A, Olsson C, Nygren O, Nilsson M, Seiving B, Cavallin-Stahl E. Pharmacokinetics and tissue distribution of cisplatin in nude mice: platinum levels and cisplatin-DNA adducts. Cancer Chemother Pharmacol. 1995;37(1):23–31.

27. Lin YS, Nguyen C, Mendoza J-L, Escandon E, Fei D, Meng YG, et al. Preclinical pharmacokinetics, interspecies scaling, and tissue distribution of a humanized monoclonal antibody against vascular endothelial growth factor. J Pharmacol Exp Ther. 1999;288(1):371–378.

28. Woodland JM, Barnett CJ, Dorman DE, Gruber JM, Shih C, Spangle LA, et al. Metabolism and Disposition of the Antifolate LY231514 in Mice and Dogs. Drug Metab Dispos. 1997 Jun 1;25(6):693–700.

29. Benzekry S, Lamont C, Beheshti A, Tracz A, Ebos JML, Hlatky L, et al. Classical mathematical models for description and prediction of experimental tumor growth. Mac Gabhann F, editor. PLoS Comput Biol. 2014 Aug 1;10(8):e1003800.

30. Skipper HE. The Effects of Chemotherapy on the Kinetics of Leukemic Cell Behavior. Cancer Res. 1965 Oct 1;25(9 Part 1):1544–50.

31. Simeoni M, Magni P, Cammia C, Nicolao GD, Croci V, Pesenti E, et al. Predictive Pharmacokinetic-Pharmacodynamic Modeling of Tumor Growth Kinetics in Xenograft Models after Administration of Anticancer Agents. Cancer Res. 2004 Feb 1;64(3):1094–101.

32. Tong RT, Boucher Y, Kozin SV, Winkler F, Hicklin DJ, Jain RK. Vascular Normalization by Vascular Endothelial Growth Factor Receptor 2 Blockade Induces a Pressure Gradient Across the Vasculature and Improves Drug Penetration in Tumors. Cancer Res. 2004 Jun 1;64(11):3731–6.

33. Hartung N, Mollard S, Barbolosi D, Benabdallah A, Chapuisat G, Henry G, et al. Mathematical Modeling of Tumor Growth and Metastatic Spreading: Validation in Tumor-Bearing Mice. Cancer Res. 2014 Nov 15;74(22):6397–407.

34. Lavielle M. Mixed Effects Models for the Population Approach: Models, Tasks, Methods and Tools. CRC Press; 2014. 385 p.

35. Li H, Takayama K, Wang S, Shiraishi Y, Gotanda K, Harada T, et al. Addition of bevacizumab enhances antitumor activity of erlotinib against non-small cell lung cancer xenografts depending on VEGF expression. Cancer Chemother Pharmacol. 2014 Dec;74(6):1297–305.

36. Nukatsuka M, Saito H, Nakagawa F, Tsujimoto H, Sakamoto K, Tsukioka S, et al. Combination therapy using oral S-1 and targeted agents against human tumor xenografts in nude mice. Exp Ther Med. 2012 May;3(5):755–62.

37. Xu Y, Chang E, Liu H, Jiang H, Gambhir SS, Cheng Z. Proof-of-concept study of monitoring cancer drug therapy with cerenkov luminescence imaging. J Nucl Med Off Publ Soc Nucl Med. 2012 Feb;53(2):312–7.

38. Winnard PT, Kluth JB, Raman V. Noninvasive Optical Tracking of Red Fluorescent Protein-Expressing Cancer Cells in a Model of Metastatic Breast Cancer. Neoplasia. 2006 Oct;8(10):796–IN1.

39. Rocchetti M, Germani M, Bene FD, Poggesi I, Magni P, Pesenti E, et al. Predictive pharmacokinetic–pharmacodynamic modeling of tumor growth after administration of an anti-angiogenic agent, bevacizumab, as single-agent and combination therapy in tumor xenografts. Cancer Chemother Pharmacol. 2013 May 1;71(5):1147–57.

40. Winkler F, Kozin SV, Tong RT, Chae S-S, Booth MF, Garkavtsev I, et al. Kinetics of vascular normalization by VEGFR2 blockade governs brain tumor response to radiation: Role of oxygenation, angiopoietin-1, and matrix metalloproteinases. Cancer Cell. 2004 Dec;6(6):553–63.

41. Dickson PV, Hamner JB, Sims TL, Fraga CH, Ng CYC, Rajasekeran S, et al.

Bevacizumab-Induced Transient Remodeling of the Vasculature in Neuroblastoma Xenografts Results in Improved Delivery and Efficacy of Systemically Administered Chemotherapy. Am Assoc Cancer Res. 2007 Jul 1;13(13):3942–50.

42. Arjaans M, Schröder CP, Oosting SF, Dafni U, Kleibeuker JE, de Vries EGE. VEGF pathway targeting agents, vessel normalization and tumor drug uptake: from bench to bedside. Oncotarget. 2016 Jan 14;7(16):21247–58.

43. Willett CG, Boucher Y, di Tomaso E, Duda DG, Munn LL, Tong RT, et al. Direct evidence that the VEGF-specific antibody bevacizumab has antivascular effects in human rectal cancer. Nat Med. 2004 Feb;10(2):145–7.

44. Van der Veldt AAM, Lubberink M, Bahce I, Walraven M, de Boer MP, Greuter HNJM, et al. Rapid decrease in delivery of chemotherapy to tumors after anti-VEGF therapy: implications for scheduling of anti-angiogenic drugs. Cancer Cell. 2012 Jan 17;21(1):82–91.

45. Collinson F, Hutchinson M, Craven RA, Cairns DA, Alexandre Z, Wind TC, et al. Biomarkers and Response to Bevacizumab—Response. Clin Cancer Res. 2014 Feb 15;20(4):1058–1058.

46. Benzekry S, Tracz A, Mastri M, Corbelli R, Barbolosi D, Ebos JML. Modeling Spontaneous Metastasis following Surgery: An In Vivo-In Silico Approach. Cancer Res. 2016 Feb 1;76(3):535–47.

47. Heist RS, Duda DG, Sahani DV, Ancukiewicz M, Fidias P, Sequist LV, et al. Improved tumor vascularization after anti-VEGF therapy with carboplatin and nab-paclitaxel associates with survival in lung cancer. Proc Natl Acad Sci. 2015 Mar 2;112(5):1547–52.

48. Lassau N, Coiffier B, Kind M, Vilgrain V, Lacroix J, Cuinet M, et al. Selection of an early biomarker for vascular normalization using dynamic contrast-enhanced ultrasonography to predict outcomes of metastatic patients treated with bevacizumab. Ann Oncol Off J Eur Soc Med Oncol. 2016 Oct;27(10):1922–8.

Tables legends

Table 1: Population parameters and inter-animal variabilities (IAV) estimates for experiment-1 data.

Figures legends

Figure 1: Scheme of the structural mathematical model

Figure 2: Efficacy and Kaplan-Meier survival curves of experiment-1

A: Mean tumor growth curves for the 4 treatment arms of experiment-1. Signs above curves indicate statistically significant difference with the control arm (Student's t-test, $p < 0.05$).

B: Kaplan Meier plot of the overall survival for the 4 treatment arms of experiment-1.

Figure 3: Visual predictive check for experiment-1 population analysis

A, B, C, D: Visual predictive check (VPC) plots. Circles: experimental data. Stars with broken lines: median data. Solid lines: tumor growth simulated curves using median parameter values, dashed lines: 95% intervals for inter-animal variability, generated from the simulation of 1000 virtual animals with parameters distributed according to the distribution estimated by the mixed-effects fit.

Figure 4: Data-informed modeling simulations of various gaps between bevacizumab and pemetrexed-cisplatin administrations

A: Median tumor growth curves.

B: Simulations of the tumor growth using different time lags between the administration of bevacizumab and pemetrexed-cisplatin (“Beva then Chemo”). The red curve corresponds to a time lag of 3 days.

C: Area under the tumor growth curve (AUC) as a function of the time lag.

D: Inter-animal variability on the optimal lag time between bevacizumab and chemotherapy (2.8 ± 1.84 days, median ± standard deviation).

Figure 5: Efficacy and Kaplan-Meier survival curves of experiment-2

A: Mean tumor growth curve for the 5 treatment arms of experiment-2. Signs above curves indicate statistically significant difference with the control arm (Student's t-test, $p < 0.05$).

B: Kaplan Meier plot of the overall survival for the 5 treatment arms of experiment-2.

Supplementary material

Supplementary methods: Parameters' estimation detailed procedure

Supplementary figures

Table 1: Parameters estimates

Parameters	Description	Units	Estimates	RSE* (%)	IAV** (%)
α	Proliferation rate	day^{-1}	0.767	8	8.62
β	Exponential decay rate of the relative tumor growth rate (Gompertz model)	day^{-1}	0.037	10	57.3
γ	Baseline effect of the chemotherapy	$(mg/g)^{-1}.day^{-1}$	1	–	–
δ	Cytotoxics efficacy improvement following vascular normalization	$(mg/mL)^{-1}$	1200	36	0
τ	Delay parameter for dynamics of Q.	day	2	20	10
k	Delay of the tumor cell loss following chemotherapy	day^{-1}	0.3	–	–
σ	Exponential error parameter	–	0.951	4	–

Values of the parameters corresponding to the adapted fit. See supplementary methods for details on the estimation procedure.

* Relative Standard Error (RSE) is a measure of the precision of the parameter estimates, expressed as coefficient of variation (CV%). ** The inter-animal variability (IAV) is the standard deviation ω estimated using Monolix software.

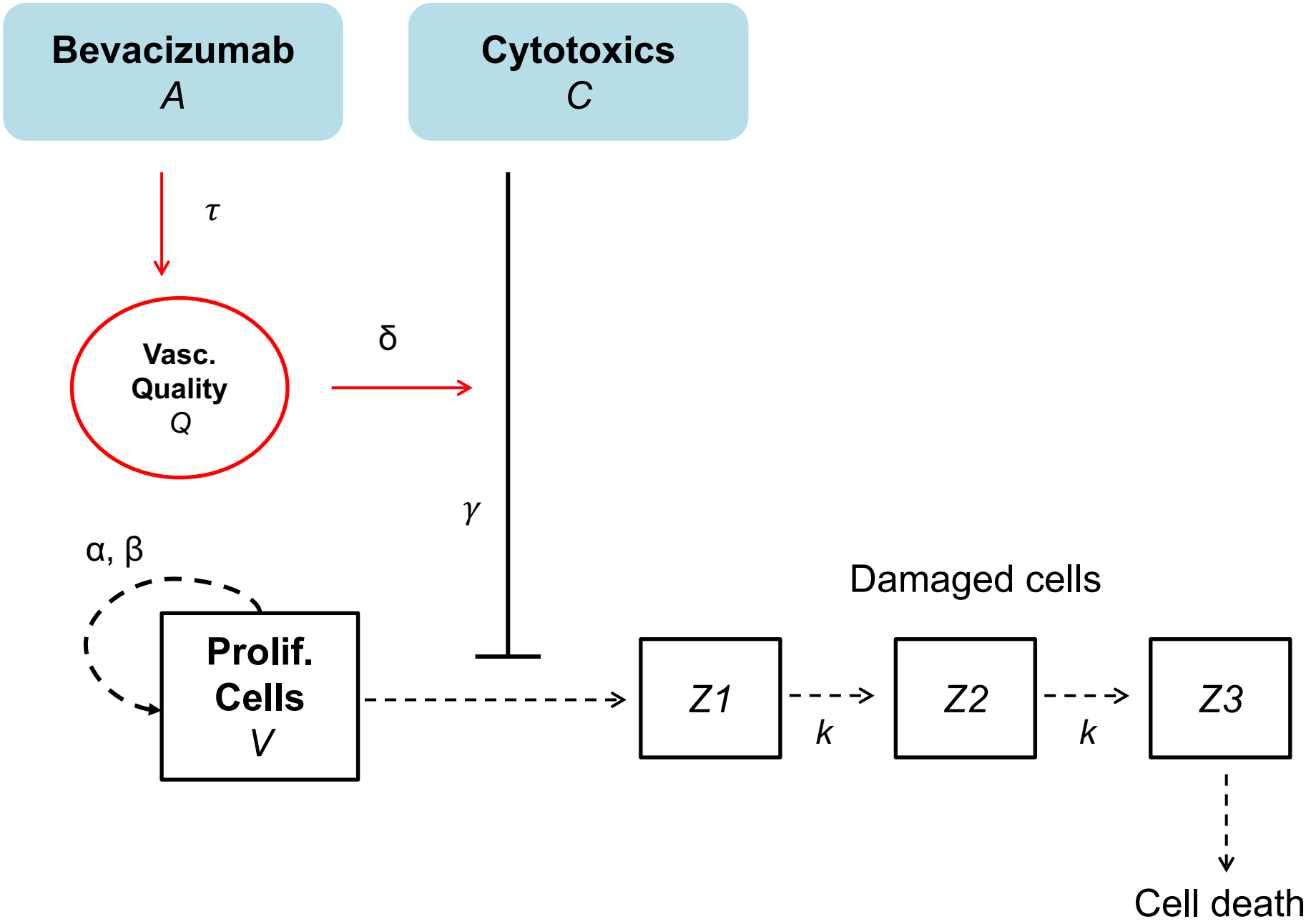
Bevacizumab
A
Cytotoxics
C
τ
Vasc.
Quality
Q
δ
γ
α, β
Prolif.
Cells
V
Damaged cells
Z1
k
Z2
k
Z3
Cell death

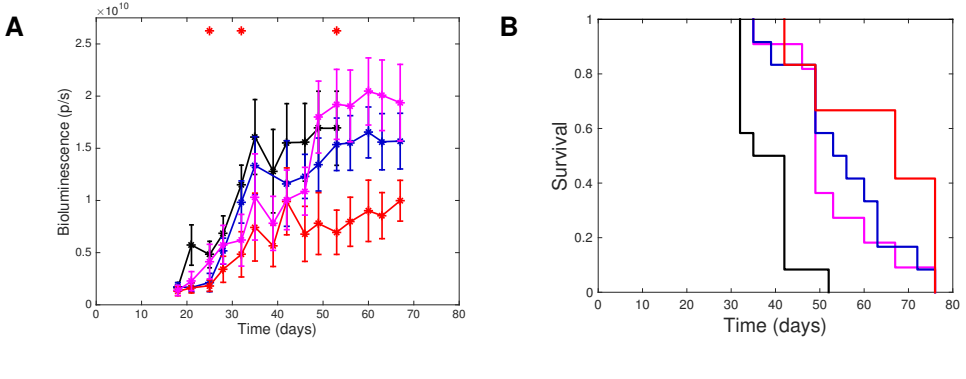
A
B
×10^10
Bioluminescence (p/s)
Time (days)
Survival
Time (days)
Control
Beva-Chemo
Beva/Chemo 4 days
Chemo/Beva 4 days

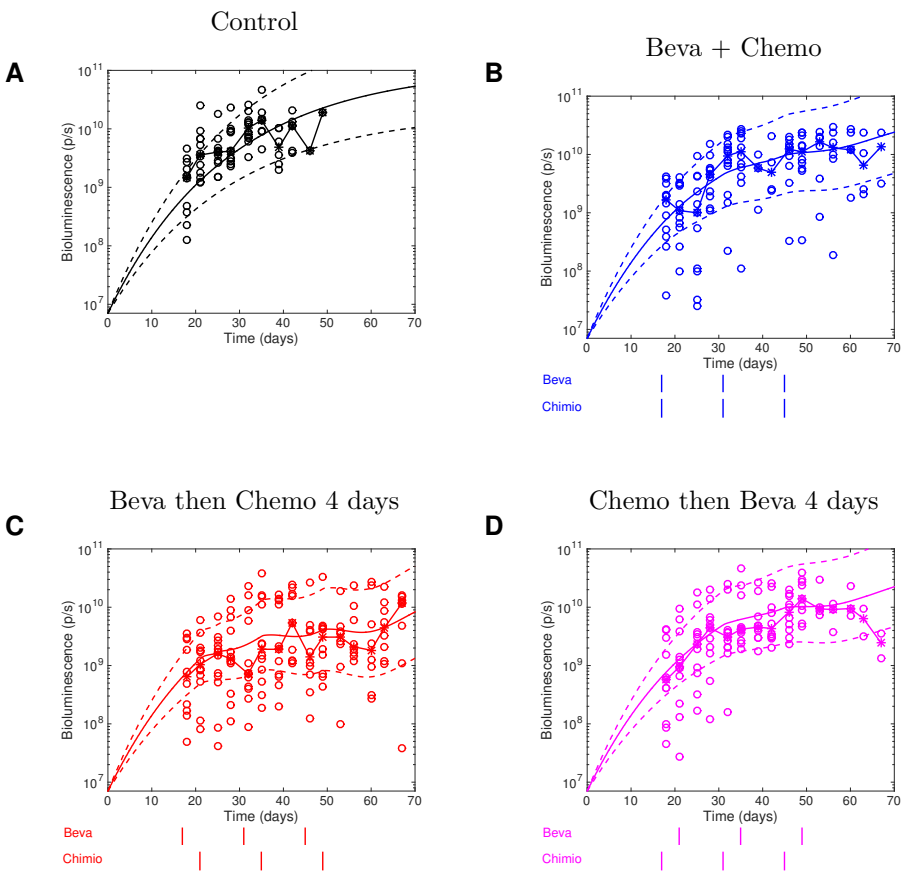
A
Control
Bioluminescence (p/s)
Time (days)
B
Beva + Chemo
Bioluminescence (p/s)
Time (days)
Beva
Chimio
C
Beva then Chemo 4 days
Bioluminescence (p/s)
Time (days)
Beva
Chimio
D
Chemo then Beva 4 days
Bioluminescence (p/s)
Time (days)
Beva
Chimio

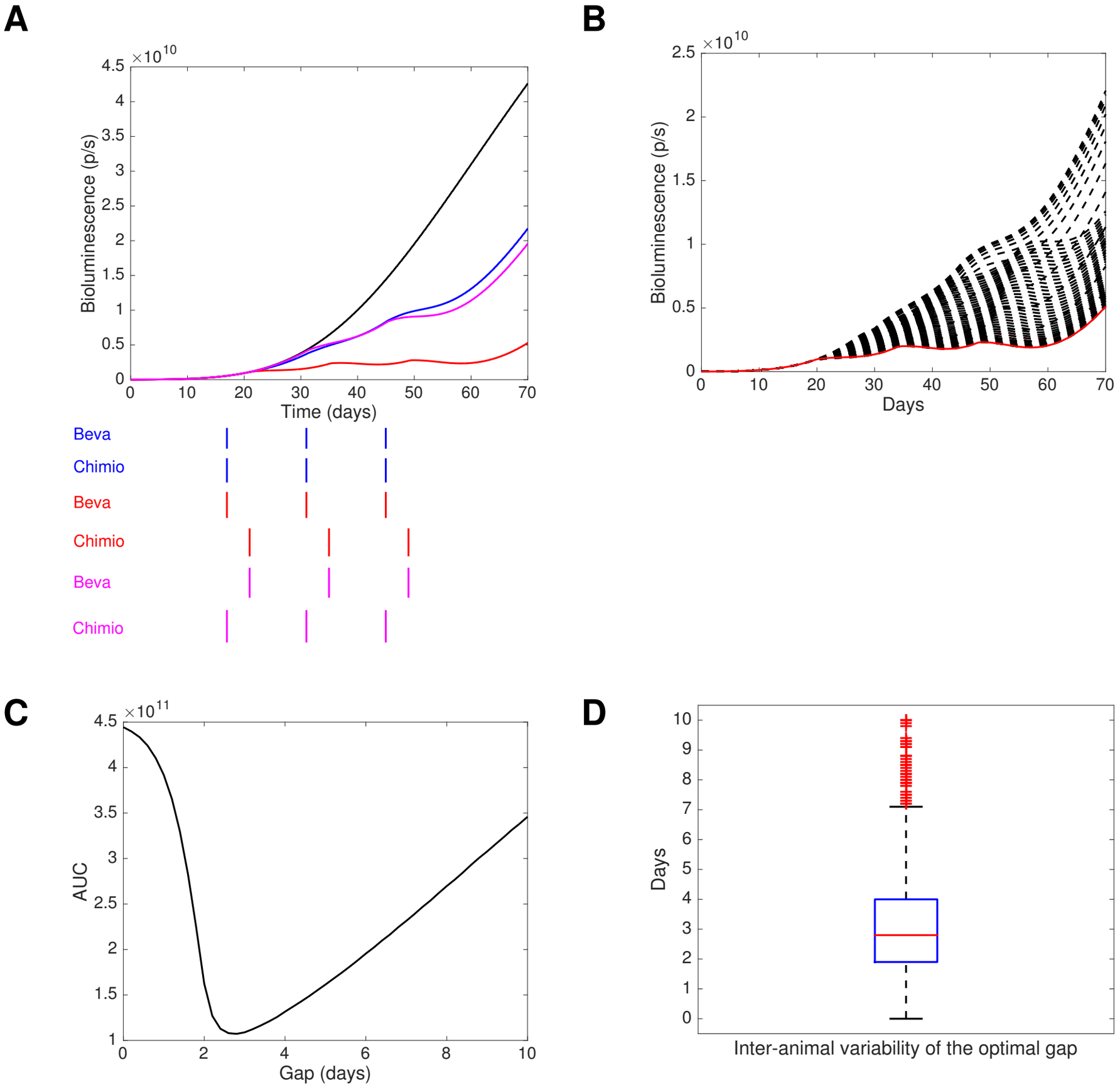
A
×10^10
Bioluminescence (p/s)
Time (days)
Beva
Chimio
Beva
Chimio
Beva
Chimio
B
×10^10
Bioluminescence (p/s)
Days
C
×10^11
AUC
Gap (days)
D
Days
Inter-animal variability of the optimal gap

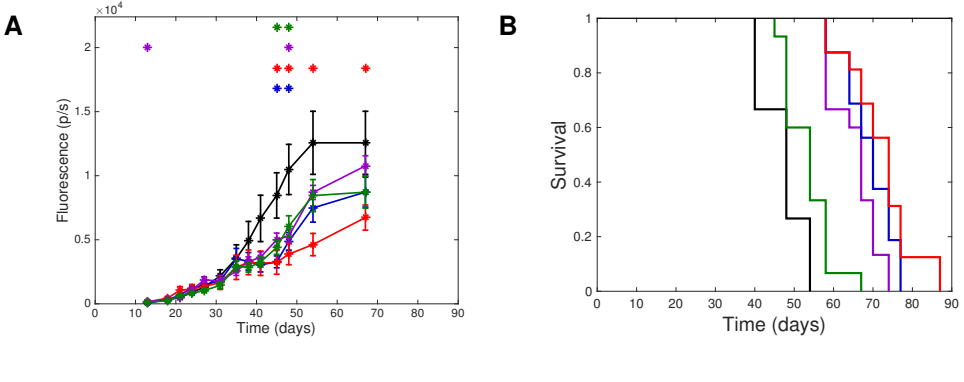
A
B
×10^4
Fluorescence (p/s)
Time (days)
Survival
Time (days)
Control
Beva-Chemo
Beva/Chemo 3 days
Beva/Chemo 8 days
Chemo

Supplementary methods for parameters' estimation

Sensitivity analysis from fits to the median data

Before running Monolix estimates for population fitting, sensitivity analyses of various model structures (i.e., either all parameters free or some fixed) were conducted. It consisted in computing the jacobian J of the model with respect to the parameters and associated standard errors of maximum likelihood estimates following the formula $Cov = \hat{\sigma}^2(J^T J)^{-1}$ for the covariance of the estimate (1), where $\hat{\sigma}$ is the estimate of the standard deviation of the error model. This applied to fits to the median data yielded important uncertainty in the estimates on γ, δ and k (respective relative standard errors of 158%, 157% and 202%) and strong correlation between parameters γ and δ (R^2=0.996), thus suggesting to fix one the two parameters γ, δ and k. Therefore, we arbitrarily fixed $\gamma = 1$ (with efficacy magnitude now only depending on δ). For the value of k, in (2), its values was estimated for multiple cytotoxic agents and ranged 0.056 - 1. After direct exploration of the model behavior for values of k in this range, we found that $k = 0.3$ was able to give a reasonable description of the data.

Likelihood maximization using the Stochastic Approximation of Expectation Maximization (SAEM) algorithm implemented in Monolix

The model then contained four parameters (and associated population standard deviation of the random effects). Likelihood maximization was performed using the Monolix software (version 2016R1, Lixoft) and an

exponential error model. To avoid possibilities of local minima, we performed different runs of the algorithm from different initial conditions and initial seeds of the stochastic algorithm. These converged to similar values of the parameters and likelihood. Taking the run yielding the largest likelihood generated a first fit to the data, with good standard errors on the parameters estimates (referred to as the "Monolix fit"). However, examination of visual predictive checks revealed a substantial discrepancy between the model fit and the data (Figure S3). The fit quality was particularly poor when looking at the median data (Figure S4). This fit seemed to under-estimate the effect of therapy δ as well as the delay τ. This was due to the presence of outliers in the data that impact the likelihood too importantly and bias the overall estimate. Indeed, as demonstrated in Figure S5, the animal that contributed the most to the likelihood in the global computation is an animal with a clear outlier.

Adapted fit

In contrast, by direct simulation of the model for varying a large range of values of parameters δ and τ (with parameters α and β from the Monolix fit since these correctly described the control data), we found values of these – referred to as the adapted fit – that exhibited a much better description of the data both at the level of visual predictive checks (Figure 3) and when comparing median simulations and the median data (Figure S6). In this process, we also found that no random effects on δ were necessary, since equally good fits were obtained setting the value of its population standard deviation to zero. Thus, in the adapted set, no random effect was assumed on δ. Further investigation revealed that although this set had a smaller log-

likelihood (-10892 vs -10886), the Monolix fit was clearly outperformed by the adapted fit when considering other statistical goodness-of-fit metrics such as the root mean squared error (RMSE). The RMSE to the median is defined, for a given group, by

$$RMSE_{med}^2 = \sum_{j=1}^{N} \frac{\left(y_j^m - \widehat{y_j^m}\right)^2}{N - p}$$

with N the number of time points, p the number of parameters of the model, y_j^m the median data at time t_j and $\widehat{y_j^m}$ the model prediction of the median (equal to $M(t_j; \hat{\theta})$ with $\hat{\theta}$ the typical parameter estimate). Another interesting metrics is the individual RMSE:

$$RMSE^2 = \sum_{i=1}^{M} \sum_{j=1}^{n_i} \frac{\left(y_{i,j} - \widehat{y_{i,j}}\right)^2}{n_i - p}$$

with M the number of animals in the group, n_i the number of time points for animal i, $y_{i,j}$ the data of animal i at time $t_{i,j}$ and $\widehat{y_{i,j}}$ its model prediction.

The RMSEs to the median were increased of 52.2%, 135% and 94% for the Monolix fit compared to the adapted fit, for the “Beva plus Chemo”, “Beva then Chemo 4 days” and “Chemo then Beva 4 days” groups, respectively. Similarly, the individual RMSEs were increased of 40.4%, 144% and 60.1% for the Monolix fit as compared to the adapted fit.

Taken together, these elements (better visual predictive check, small difference to the maximal likelihood and clear superiority for RMSEs) support the adapted fit values of the parameters as a more faithful description of our data than the Monolix fit.

References

1. Seber GA, Wild CJ. Nonlinear regression. Wiley-Interscience; 2003.

2. Simeoni M, Magni P, Cammia C, De Nicolao G, Croci V, Pesenti E, et al. Predictive pharmacokinetic-pharmacodynamic modeling of tumor growth kinetics in xenograft models after administration of anticancer agents. Cancer Res. 2004 Feb 1;64(3):1094–101.

Supplementary Figures

Figure S1: Design of experiments -1 and -2

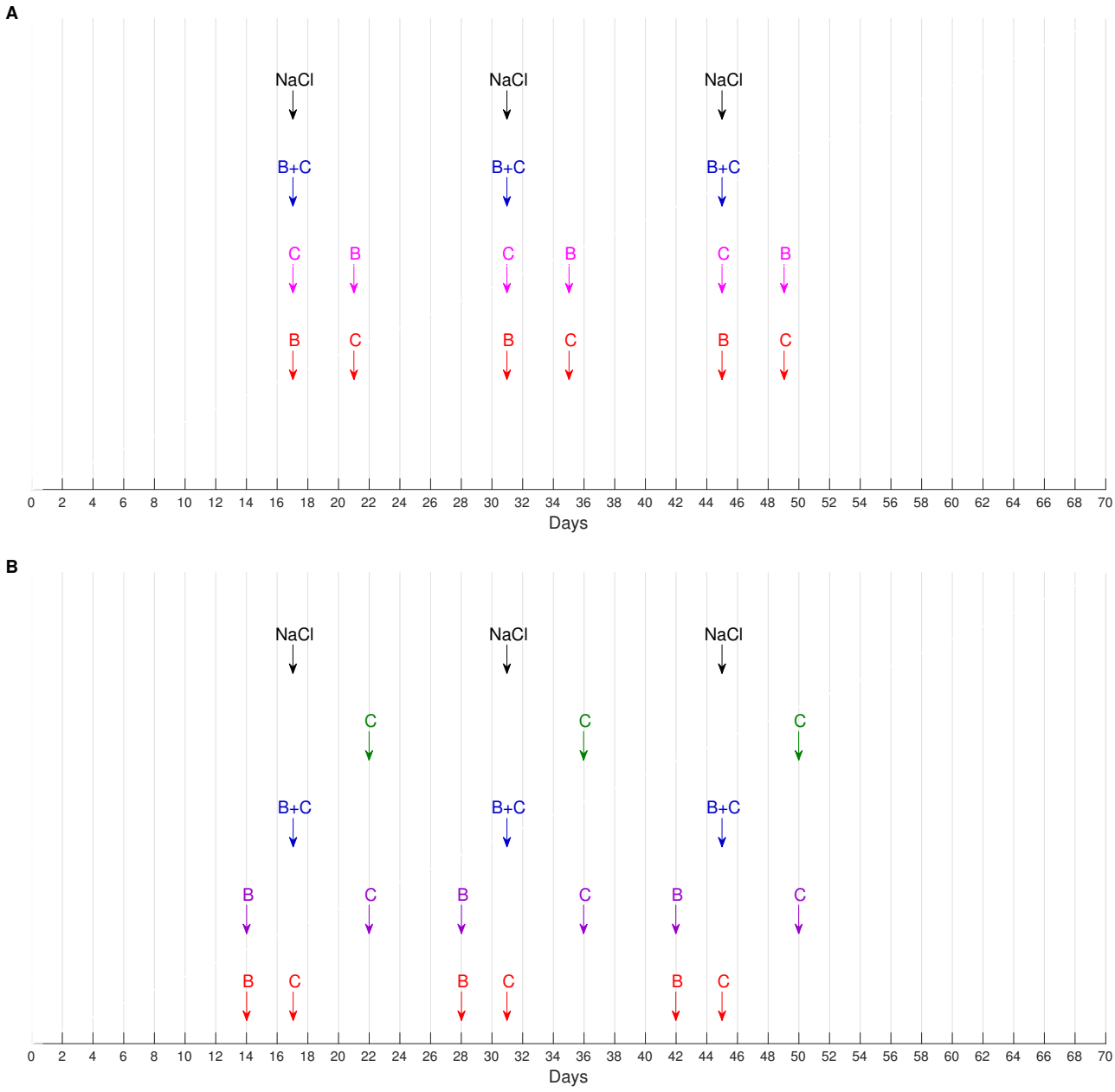

Arrows indicate administration time.
A- Experiment-1 : Black arrows: Control group. Blue arrows: Concomitant group (”Beva + Chemo”). Magenta arrows: Reversed group with cytotoxics administered 4 days before bevacizumab (”Chemo then Beva 4 days”). Red arrows: Sequential group with bevacizumab administered 4 days before cytotoxics (”Beva then Chemo 4 days”).

B- Experiment-2 : Black arrows: Control group. Green arrows: Cytotoxics only group (Chemo). Blue arrows: Concomitant group (”Beva + Chemo”). Purple arrows: Aberrant sequential group with bevacizumab administered 8 days before cytotoxics (”Beva then Chemo 8 days”). Red arrows: Optimized sequential group with bevacizumab administered 3 days before cytotoxics (”Beva then Chemo 3 days”)

Figure S2: Pharmacokinetic profiles

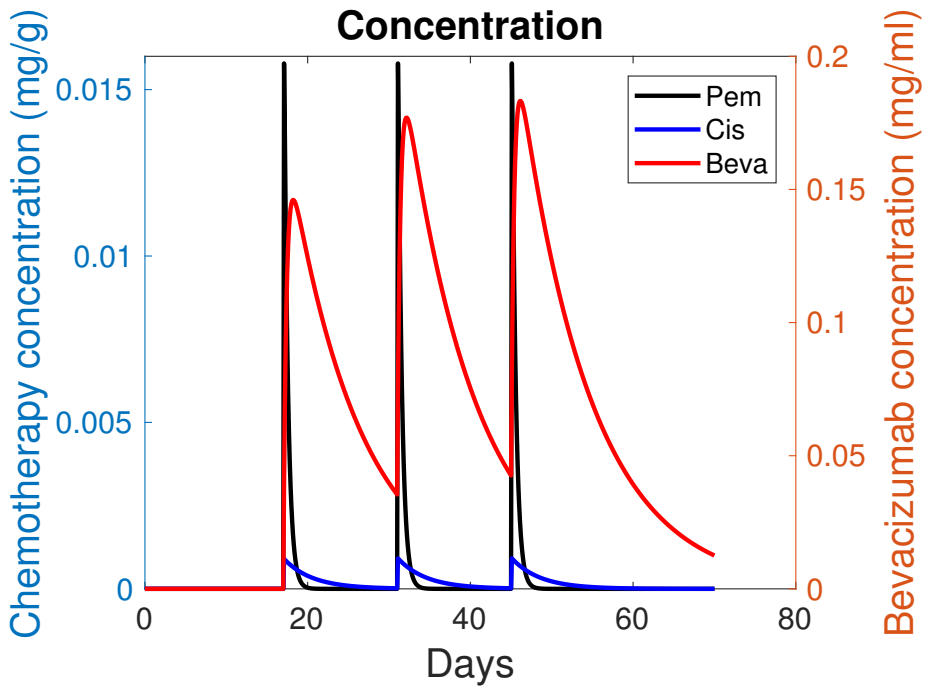

Pharmacokinetics profile of bevacizumab (red line), pemetrexed (black line) and cisplatin (blue line) for 3 treatment cycles (intra-peritoneal injections of 20, 100 and 3 mg/kg for bevacizumab, pemetrexed and cisplatin respectively).

Figure S3: Visual predictive checks of the Monolix fit

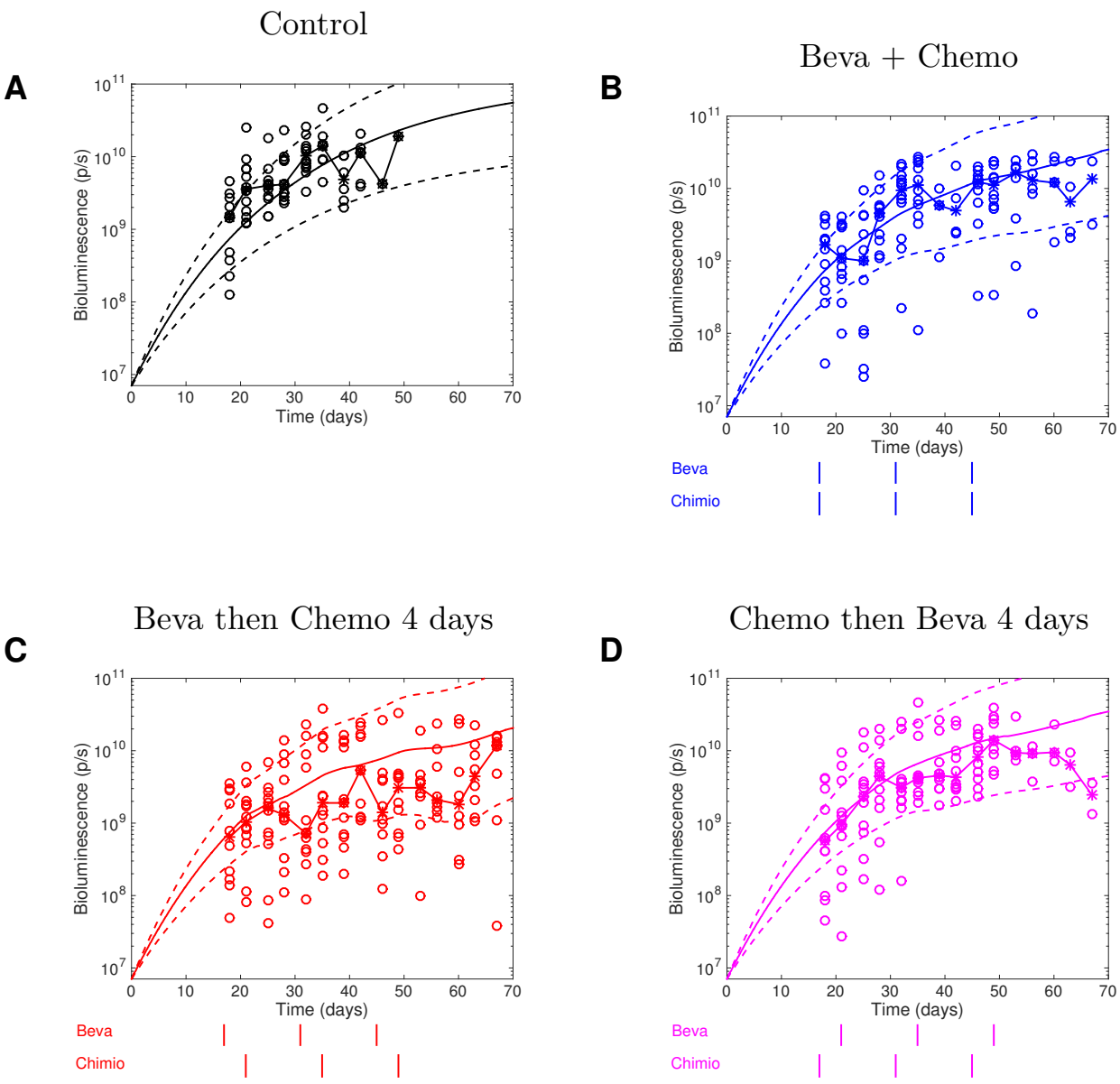

Visual predictive checks of the initial Monolix fit shows lack of descriptive power, especially for the “Beva then Chemo 4 days” group.
Circles: experimental data. Stars with broken lines: median data. Solid lines: tumor growth simulated curves using median parameter values, dashed lines: 95% intervals for inter-animal variability, generated from the simulation of 1000 virtual animals with parameters distributed according to the distribution estimated by the mixed-effects fit.

Figure S4: Monolix fit vs median data

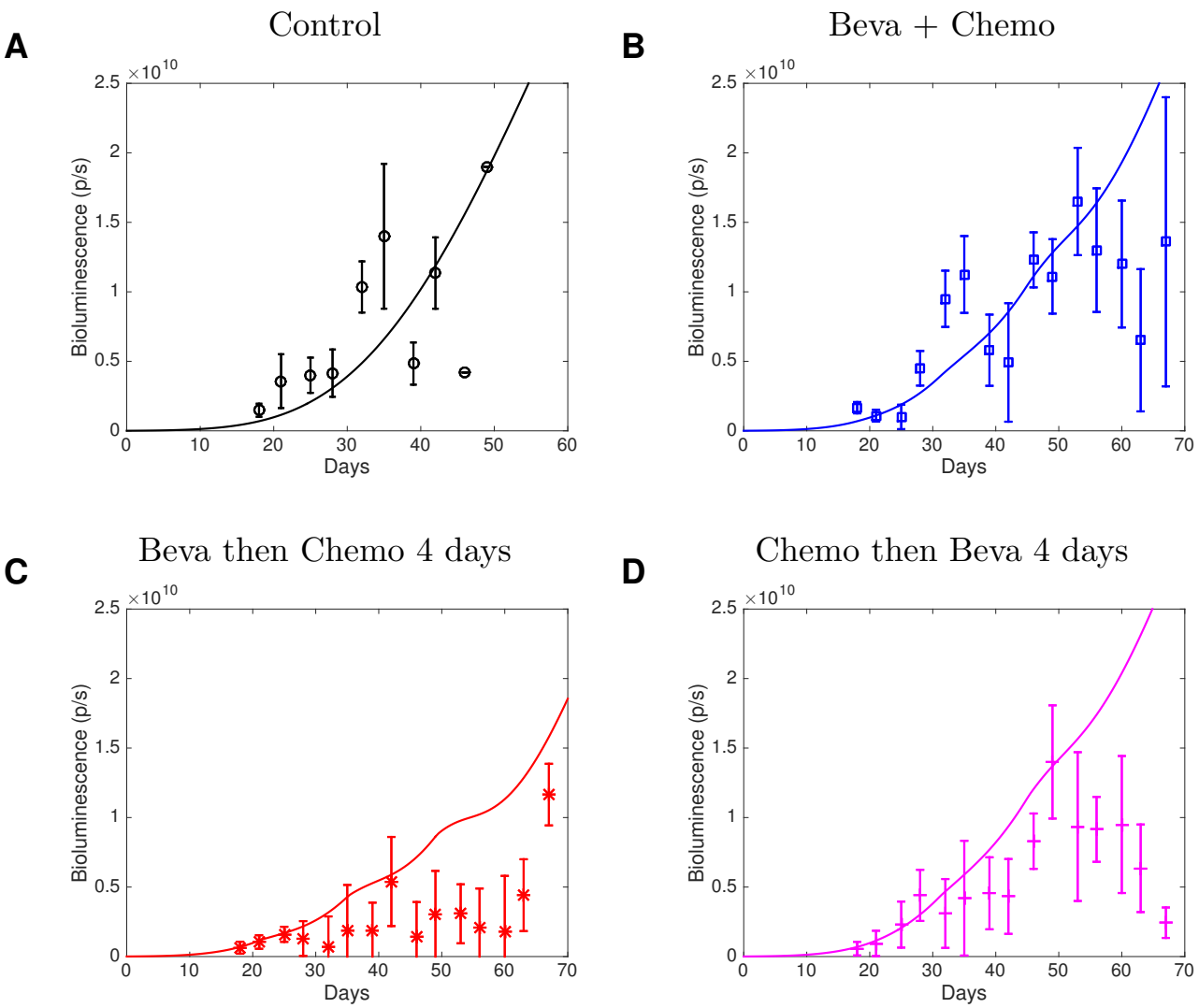

Figure S5: Individual fits of the animal that had the most important contribution to the likelihood

Monolix fit | **Adapted fit**

Animal 8 Beva then Chemo 4 days

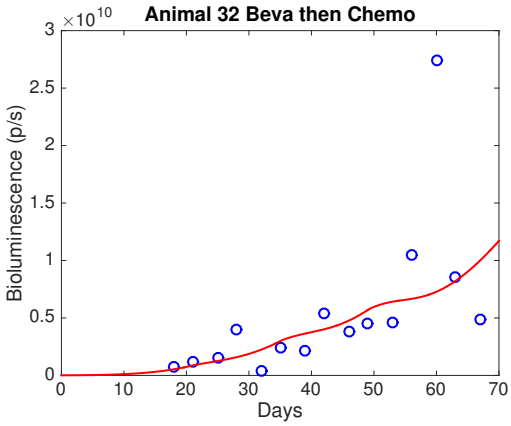

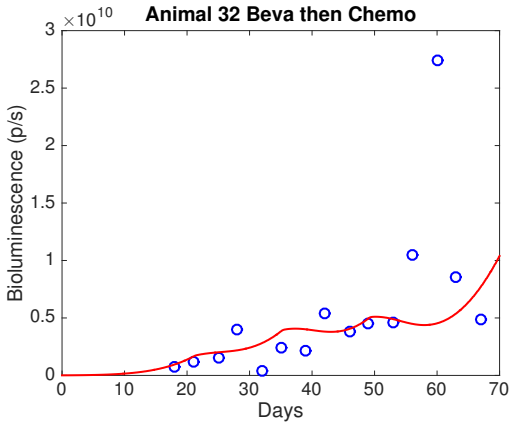

Figure S6: Adapted fit vs median data

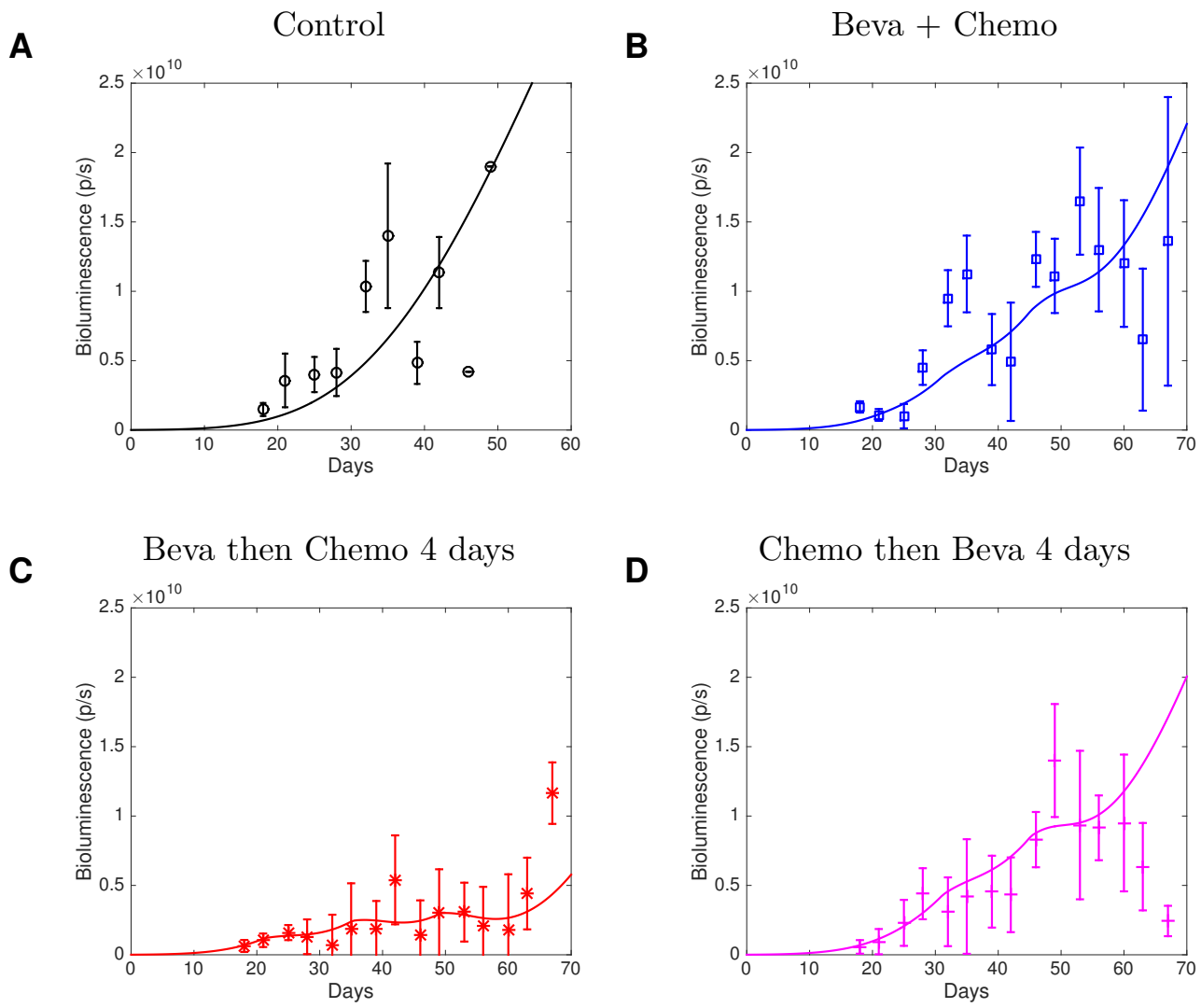

Figure S7: Residual analysis for experiment-1 population analysis

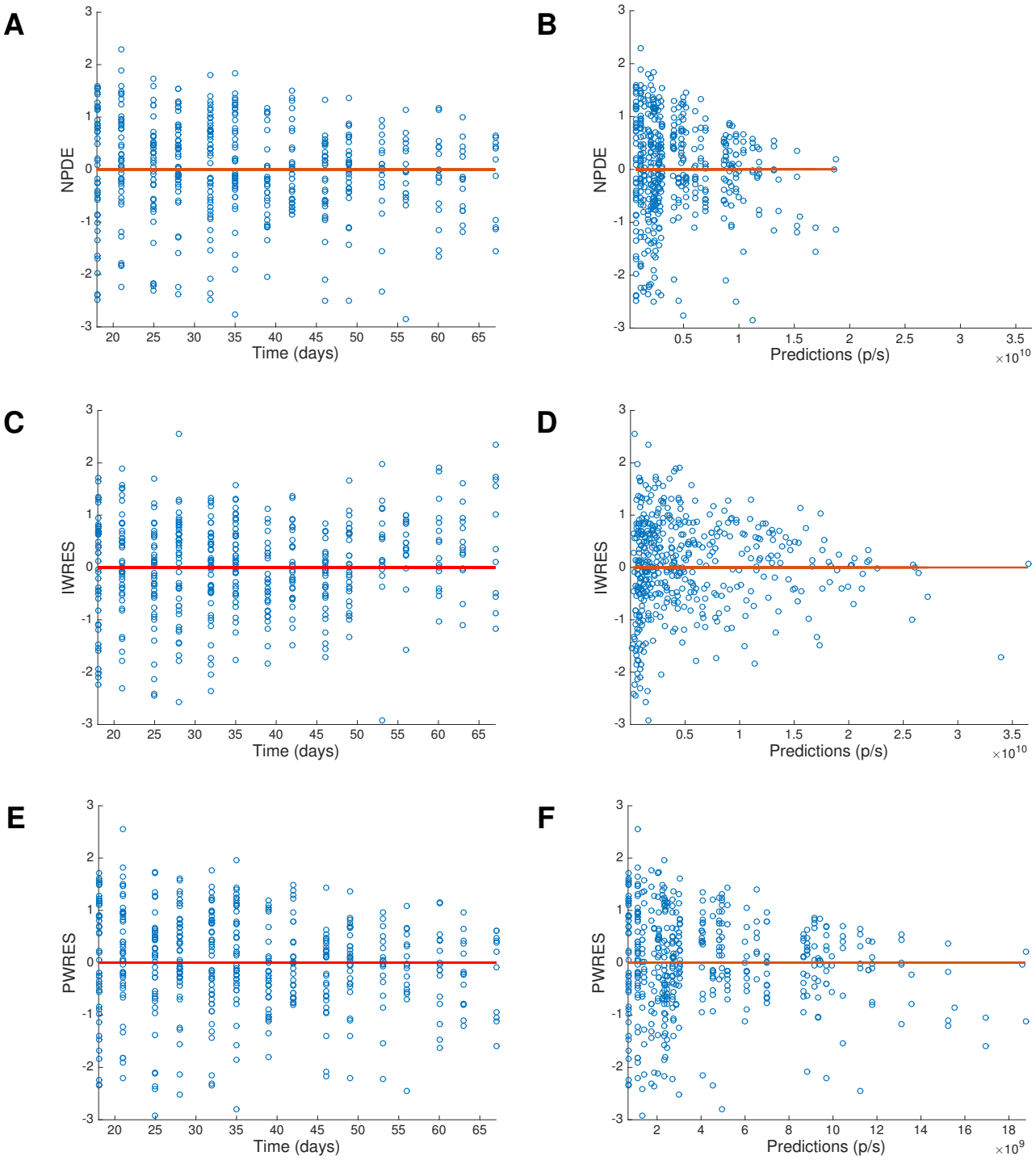

A- Normalized Predictions Distribution Errors (NPDE) *vs.* time
B- Normalized Predictions Distribution Errors (NPDE) *vs.* predictions
C- Individual Weighted Residuals (IWRES) *vs.* time
D- Individual Weighted Residuals (IWRES)*vs.* predictions
E- Population Weighted Residuals (PWRES) *vs.* time
F- Population Weighted Residuals (PWRES) *vs.* predictions
Plots were generated using residuals exported from Monolix.

Figure S8: Individual tumor growth simulations

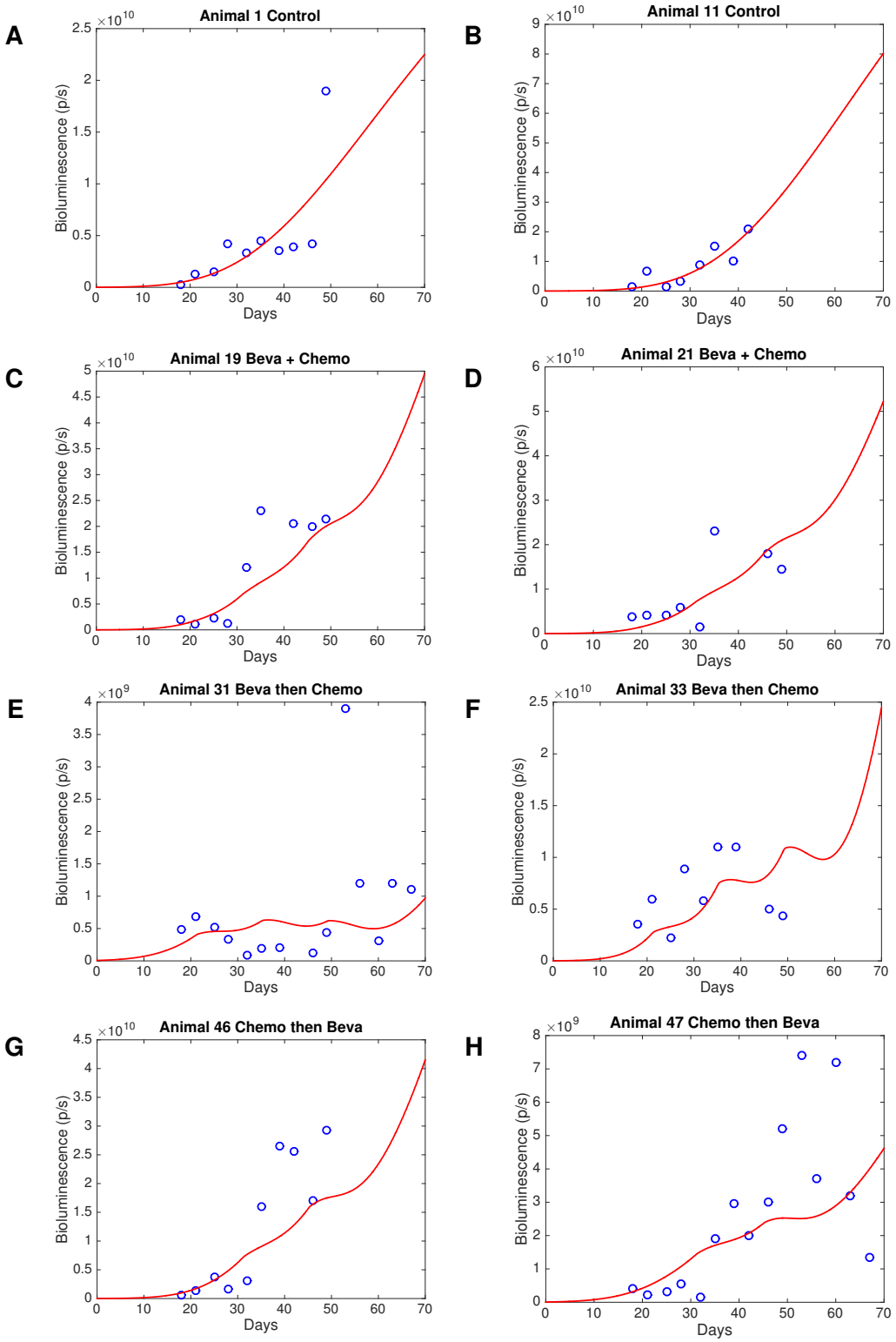

Individual tumor growth simulations of random subjects from experiment-1.
Blue circles: experimental data. Red lines: simulated tumor growth curves